Cooperative Micelle Binding and Matrix Effect in Oleate Vesicle Formation

Silvia Rasi, Fabio Mavelli, and Pier Luigi Luisi*

Institute of Polymers, Swiss Federal Institute of Technology (ETH-Z), Zürich, Switzerland

Received: December 14, 2002; In Final Form: August 3, 2003

Kinetics and particle size distributions in the spontaneous micelle−vesicle transformation of oleate vesicles are investigated by dynamic light scattering and optical density measurements. It is shown that, depending upon the conditions, there are two different kinetic processes for vesicles formation, a cooperative and a uncooperative one. In particular, the time progress of vesicle formation follows a sigmoid behavior and it is accelerated by the presence of preformed vesicles, confirming that a cooperative micelle−vesicle interaction takes place. This effect is investigated by adding fresh oleate surfactant to preformed, extruded (50 and 100 nm) oleate vesicles as well as to 50 and 100 nm extruded POPC (POPC is 1-palmitoyil-2-oleyl-*sn*-glycero-3-phosphocholine) liposomes. It is shown that both in the case of oleate and POPC the rate process of vesicle formation is remarkably accelerated with respect to the control (no preformed vesicles); and the final size distribution is very close to the narrowly distribution curve of the preformed vesicles, whereas in the control experiment (no preadded vesicles) a very broad distribution is obtained. We called this phenomenon the *matrix effect* to stress that preexisting vesicles or liposomes act as a matrix on the formation of the new ones. The time evolution of the particles average radius after addition of fresh surfactant is followed by means of the dynamic light scattering cumulant analysis, and thus when oleate micelles are added to oleate vesicles, a slight increase of the average dimensions is observed, whereas in the case of oleate added to POPC liposomes, the final radius is actually smaller than the initial radius. This confirms that under certain conditions, fission of vesicles is possible. Finally, some theoretical considerations on the kinetics of the micelle−vesicle cooperative transformation are drawn.

Introduction

During the last years we have studied in some detail the aggregates formed by fatty acids such as caprylic,[1] methyl dodecanoic,[2] and oleic acid,[3] including giant vesicles obtained from oleic acid.[4] There are several reasons for this interest. First, these vesicles are examples of spontaneous vesiculation; i.e., they form by simple addition of the surfactant in water.[5] Furthermore, thanks to the possibility of synthesizing easily these surfactant molecules from water-insoluble precursors, micelles and vesicle self-reproduction systems could be developed.[1,6] In addition, the fast and rapid uptake of monomer oleate by oleate vesicles as well as by POPC liposomes (i.e., vesicles formed by lipids) permits to study the mechanism of vesicles growth and fission.[7,8]

In this work we will focus attention on the transition from oleate micelles (OM) to oleic acid/oleate vesicles (OAV), a transition induced by a pH change. It is well-known that oleate micelles are promptly formed in water and are stable above the Kraft temperature and the critical micelle concentration[9] if the solution pH is higher than 10.5.[9,10] By decreasing pH, vesicles start to form in the micellar solution up to a pH value of 8.0.[9−11] As reported in a previous work,[7a] if an aqueous solution of oleate micelles is added to water buffered solution at pH 8.5, unilamellar oleate/oleic acid vesicles form spontaneously due to the pH change. The vesicles prepared in this way present a very broad size distribution. By contrast, the addition of the same OM solution volume to a OAV suspension with a very narrow size distribution results in a final vesicle size distribution that is very close to the initial one.[7] Moreover, in the presence of preformed OAV the micelle−vesicle transformation is faster than in their absence, as judged by the time progress of the increase of the optical density or of scattered light intensity at 90°. We have called this phenomenon the *matrix effect* to indicate that the preexisting organized material acts as a matrix for the newly formed vesicles. This effect can be due to a cooperative micelle binding to vesicles, as suggested by the sigmoid optical density time progress and by the acceleration of the micelle transformation in the presence of preadded vesicles. To understand this feature, consider first that a sigmoid behavior is an indication of an autocatalytic cooperative mechanism.[1,6] According to this view (see Figure 1 for a pictorial representation) the initial vesicles form with difficulty (initial lag phase), but once the first ones are formed, further micelle transformation is made easier. This is due to the fact that the surfactant binds to the formed vesicles (cooperative binding), which grow and eventually split, giving rise to more vesicles. These, in turn, permit the binding of more of the fresh surfactant, which in turn induces more new vesicles. Evidence for this mechanism has been recently obtained also by electron microscopy, using ferritin-labeled oleate and POPC vesicles.[8] Alternatively, as illustrated in Figure 1, the fresh added surfactant could self-assemble into vesicles without interaction with the previously freshly formed vesicles. Can one demonstrate further that the sigmoid trend is due to an autocatalytic process?[12] This can be done by arguing as in our previous work:[1,4] if the lag phase is due to the difficulty of building the first vesicles, the presence of preformed vesicles should decrease the lag phase and accelerate further the overall process. This is indeed what happens, as schematically illustrated in Figure 1, where the optical density time progress in the presence of a cooperative

10.1021/jp0277199 CCC: $25.00 © 2003 American Chemical Society
Published on Web 11/19/2003

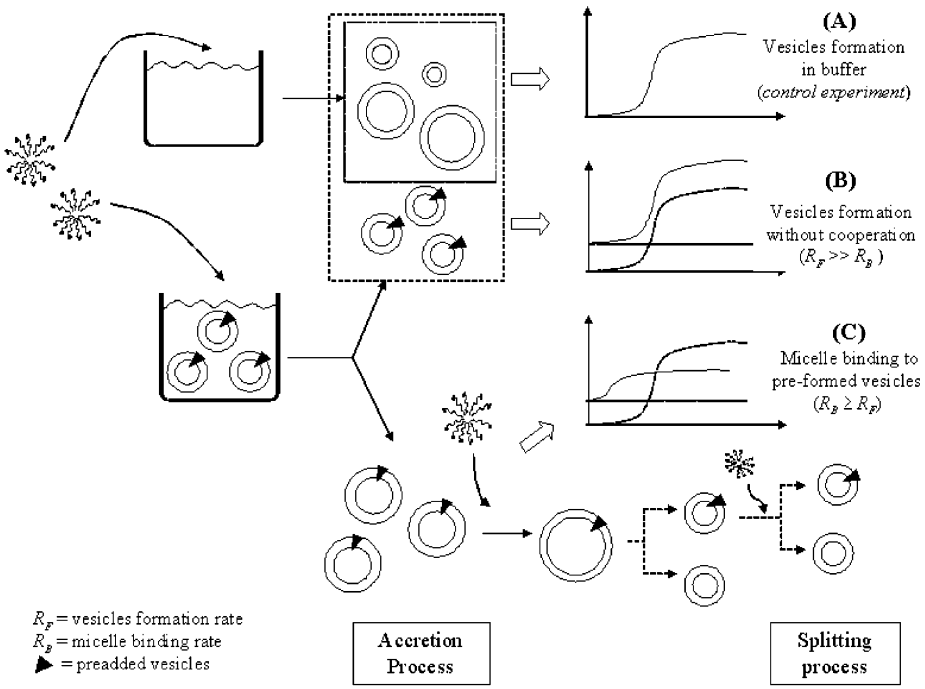

Figure 1. Hypothetical mechanism of the oleate micelle−vesicles transition in buffer (case A) and in the presence of preadded vesicles (cases B and C). After surfactant addition to a preformed vesicle suspension the micelle−vesicles transition could occur by two different mechanisms: (1) added micelles do not interact with the preexisting vesicles (case B) and the optical density time progress should be similar to that observed in the control experiment (case A); (2) added amphiphiles are first absorbed by the preadded vesicles (cooperative binding) following a growth in size and possibly a division with formation of smaller aggregates (case C). The process is faster than adding amphiphiles only to the buffer. The solid triangular markers indicate the preexisting vesicles.

micelle binding (case C) is compared with a uncooperative vesicle formation (case B).

All these are novel and partly unexpected features that require further investigations. The present paper is focused on the following points: (i) the influence of parameters such as buffer and ionic strength on the mechanism of self-reproduction of oleate vesicles; (ii) the matrix effect observed upon the addition of fresh oleate monomer to preformed oleic−oleate vesicles and POPC liposomes, looking in particular at the influence of the dimensions of the preadded liposomes on the rate of formation and final size distribution of the final mixed vesicles; (iii) theoretical support to the mechanism proposed for the oleic−oleate vesicles formation, in particular for the cooperative binding.

Materials and Methods

Chemicals. Sodium oleate (>99%), oleic acid (puriss, standard for gas chromatography), boric acid (>99.5%), bicine (>99.5%), and sodium chloride (>99.5%) were from Fluka, Buchs, Switzerland, and used as received. POPC was from Avanti Polar Lipids, Alabaster, AL.

Buffer Preparation. The 0.22 M bicine and borate buffer solutions were prepared by dissolving bicine and boric acid in ultrapure water and adjusting the pH with 1 M NaOH to pH 8.5. The ionic strength value and the amount of salt added were calculated by the formula:

$$I = {}^1/_2 \sum_i z_i^2 C_i$$

where z_i is the charge number of an ion i and C_i is the molar concentration. To study the influence of the ionic strength, the bicine buffer was first diluted up to the concentration 0.0178 M and $I = 0.011$ M and then the ionic strength was increased by adding NaCl up to the value $I = 0.127$ M.

In the case of borate the buffer at higher ionic strength was just prepared by adding NaCl up to $I = 0.127$ M.

Oleic Acid/Oleate Vesicles. Vesicles composed of oleate/oleic acid were prepared by dispersing 0.0282 g of oleic acid in 0.22 M bicine buffer (0.22 M, pH 8.5, 5 mL) under magnetic stirring at room temperature overnight.

POPC Liposomes. POPC liposomes were prepared by dissolving 0.0760 g of POPC in chloroform (3 mL) in a 50 mL round-bottom flask. This mixture was shaken for some minutes at room temperature to obtain a homogeneous solution. The solvent was then removed by evaporation using a rotary evaporator ($p = 400$ mbar, $T = 25$ °C) until the formation a lipid film. After drying under vacuum overnight, the residual lipid film was hydrated with a defined volume of bicine buffer solution (0.22 M, pH 8.5, 5 mL).

Vesicles and Liposomes Extrusion. To form 100 and 50 nm unilamellar spherical sized vesicles or liposome suspensions, a 5-times freeze−thaw cycle (freezing the suspension in liquid nitrogen and thawing at room temperature) was first applied to reduce lamellarity,[13] followed by 10-times passage through polycarbonate membranes of decreasing pore sizes (400−200−100 and 400−200−100−50 nm diameters, respectively). "The Extruder" from Lipex Biomembranes (Vancouver, Canada) was used, whereas the Nucleopore polycarbonate membranes were obtained from Sterico AG, Dietikon, Switzerland.

Addition of Oleate Micelles to Buffer Solutions and Preformed Aggregates Suspensions. An aqueous micellar solution (22 mM) was prepared by dissolving sodium oleate in ultrapure water. A 200 μL aliquot of this freshly prepared solution was directly injected into a spectrophotometric cell by a 250 μL Hamilton syringe equipped with a 50.0 mm long blunt needle (o.d. 0.72 mm, i.d. 0.41 mm, volume 3.35 μL/inch). The cell was filled with the bicine buffer solution (control experiment) or with 2.0 mL of a 2.2 mM surfactant concentration

extruded vesicles−liposomes suspension. The cell was then gently shaken by hand before measuring. Notice the overall surfactant concentration is 2.0 mM in the control experiment, whereas it is doubled in the presence of preadded aggregates.

Optical Density (OD) Measurements. OD measurements were carried out at 400 nm, 25.0 ± 0.1 °C, with a Cary 1E UV/vis multicell spectrophotometer from Varian using quartz cells with a path length of 1 cm.

The time progress of the optical density will be used to monitor the formation of vesicles and in this regard one should keep in mind that the optical density OD is a complex property that in the case of particles of any sizes and shape can be expressed by[14]

$$2.303\ \mathrm{OD} = 2\pi N_p \int_0^{\pi} j(q)\,\sin(q)\,\mathrm{d}q$$

where N_p is the number of particles per cm^3, q is the scattering angle, $j(q)$ is the Rayleigh ratio for unit intensity and depends on the wavelength of incident beam in the medium, on the relative refractive index, on the form factor, and on the square of the particle volume.

Dynamic Light Scattering. Liposome size distributions were obtained by dynamic light scattering (DLS; also called Photon Correlation Spectroscopy, PCS). The measurements were carried out by a Zetasizer 5000 (Malvern Instruments, Malvern, U.K.) consisting of a photomultiplier tube, a Malvern 7132 multibit digital correlator, and a 5 mW He−Ne laser (λ = 633 nm). The scattering cell was thermostated at 25.0 ± 0.1 °C. All the experiments were performed at the scattering angle 90°; other settings were: solvent viscosity 0.899 mPa s, solvent refractive index 1.33. Hydrodynamic average radius and intensity weighted size distribution were calculated by the cumulant[15] and CONTIN method,[16] respectively, using programs provided by the manufacturer. The cumulant analysis was performed by gathering the intensity autocorrelation function over duration of 1 min, and the mean hydrodynamic radius was calculated according to the Stokes−Einstein relationship.[17] Great care was taken to avoid the presence of dust in every step of the vesicles preparations, which were analyzed without any pretreatment.

Results and Discussion

Influence of Ionic Strength on the Kinetics of Vesicle Formation. In this first section we study the influence of two different buffers and of the ionic strength on the micelle−vesicle transformation. The general procedure is to add aliquots of a concentrated oleate stock aqueous solution (pH = 10.5) to a bicine buffer solution and a borate buffer solution at a pH = 8.5, up to a final concentration of the surfactant of 2 mM

Let us now consider Figure 2A,B that compare the OD time courses of vesicle formation for the bicine (Figure 2A) and the borate (Figure 2B) buffers at different ionic strength values and at room temperature. Notice that the time process at high ionic strength is much more sigmoid, than at low ionic strength; second, the final optical density at low ionic strength is quite lower than the one at high ionic strength.

Thus, one possible explanation for the data of Figure 2A,B might be the following: independently of the used buffer by decreasing the ionic strength, i.e., the polarity of the medium, the formation of first vesicles becomes faster and the lag phase practically disappeared. On the other hand, at high salt concentration the doubled charged layer around micelles becomes thicker and this diminishes the electrostatic repulsion and accelerates the micelle binding to vesicles. As a consequence, at low ionic strength more vesicles are rapidly formed

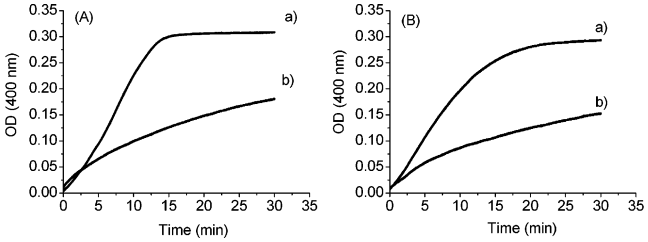

Figure 2. Effect of the ionic strength on the time progress of optical density OD variation monitored by spectrophotometry (λ = 400 nm, 25 °C). In (A) 200 μL of sodium oleate in water (22 mM) is added to 2.0 mL of bicine buffer 0.0178 M pH = 8.5 (oleic−oleate final concentration = 2 mM) at high ionic strength 0.127 M (curve a) and low ionic strength 0.011 M (curve b). The first 30 min. In (B) 200 μL of sodium oleate in water (22 mM) is added to 2.0 mL of borate buffer 0.22 M pH = 8.5 (oleic−oleate final concentration = 2 mM) at high ionic strength 0.127 M (curve a) and low ionic strength 0.031 M (curve b). The first 30 min.

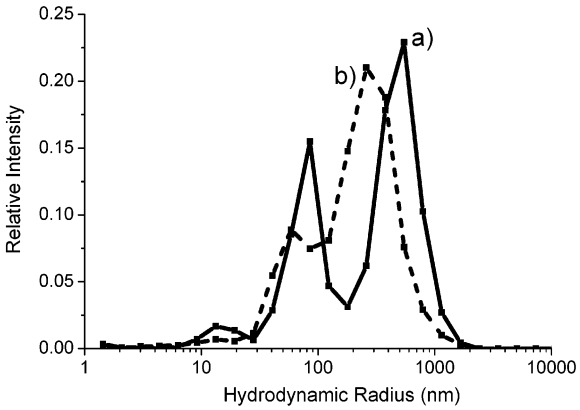

Figure 3. Effect of the ionic strength on intensity-weighted size distribution (scattering angle 90°, 25 °C) after injection of an aqueous sodium solution into borate buffer. A 200 μL aliquot of sodium oleate in water (22 mM) is added to 2.0 mL of borate buffer 0.22 M pH = 8.5 (final concentration oleic−oleate = 2 mM) at high ionic strength 0.127 M (curve a) and at low ionic strength 0.031 M (curve b). Logarithmic scale in x axis.

that grow more slowly, whereas at high ionic strength few vesicles are slowly formed that grow more rapidly, reaching higher sizes, as indicated by the OD final values. This is also confirmed by Figure 3, where the relative intensity size distributions obtained by DLS measurements at different ionic strength values are reported in the case of borate buffer. The samples have been collected after ca. 60 min, i.e., after reaching the plateau in the low ionic strength data (see Figure 2A). The difference between the various plateau values remains the same as after 30 min. The size of the vesicles range between ca. 10 nm and 1 μm, and clearly in the case of high ionic strength the distribution is shifted toward quite larger average radii.

This simple argument can indeed be an explanation for the results, however, by increasing the ionic strength over a certain value, a more complex behavior can be observed (data not shown), which is now under study in our group. This is probably due to the fact that the presence of added salts can also influence the stability and the size distribution of vesicles.

Matrix Effect. Let us consider now the formation of vesicles in the presence of vesicles already present in the aqueous solution. As already mentioned, we have used this type of experiment in previous work, arriving at the so-called matrix effect. By this we mean that the size distribution as well as the velocity of formation of new vesicles is determined by the presence of the preformed ones. In particular, under certain

TABLE 1: Mean Hydrodynamic Radius before and after Micelle Addition, Population Index f_N, and Size Index f_R[a]

solution	filter pore o.d. (nm)	before micelle addition		1.5 h after micelle addition			
		$\bar{R}$ (nm)	σ (nm)	$\bar{R}$ (nm)	σ (nm)	f_N	f_R
bicine buffer				268 ± 9	239 ± 9		
oleic acid/oleate vesicles	50	35.0 ± 0.8	12.5 ± 2.0	47.7 ± 0.8	20.0 ± 4.0	0.03	0.94
	100	46.3 ± 0.8	15.0 ± 2.3	58.1 ± 1.0	22.3 ± 2.1	0.22	0.64
POPC liposomes	50	38.4 ± 0.2	6.6 ± 0.7	36.6 ± 2.0	10.2 ± 5.1	1.15	−0.10
	100	52.5 ± 0.2	10.9 ± 0.9	48.7 ± 3.0	13.7 ± 1.9	1.37	−0.22

[a] Each radius was determined by DLS (cumulant analysis) as the mean value of 3 different experiments. In each experiment 200 μL sodium oleate solution (22 mM) were injected into extruded preformed vesicles (final total concentration 4.0 mM) and into bicine buffer 0.22 M pH = 8.5 (final concentration 2 mM). The indices were calculated by eqs 1 and 2.

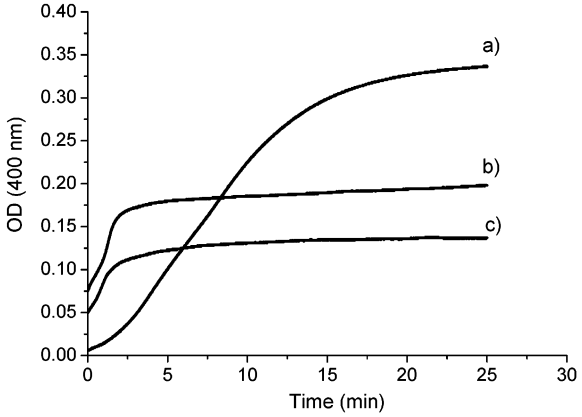

Figure 4. Effect of extruded preadded oleate/oleic acid vesicles on the oleate micelle transformations. The variation of OD after oleate micellar injection into preexisting vesicles is measured by a spectrophotometer (λ = 400 nm, 25 °C). A 200 μL aliquot of sodium oleate aqueous solution (22 mM) is injected into bicine buffer 0.22 M, pH = 8.5 (final surfactant concentration = 2 mM, curve a). The same micellar solution is injected into 100 nm (curve b) and 50 nm (curve c) extruded oleic vesicle suspensions (2.2 mM; final total concentration after injection = 4.0 mM).

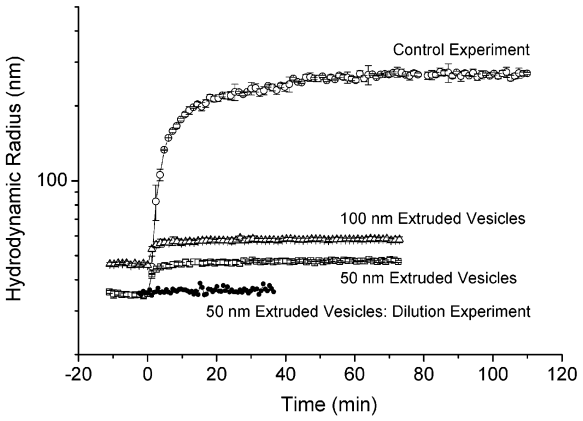

Figure 5. Time progression of hydrodynamic radius before and after injection of oleate micellar solution into extruded preadded oleate/oleic acid vesicles. The radius is measured by DLS (λ = 633 nm, scattering angle 90°, 25 °C). A 200 μL aliquot of sodium oleate aqueous solution (22 mM) is injected into bicine buffer 0.22 M, pH = 8.5 (final surfactant concentration = 2 mM, control experiment). The same micellar solution is injected into 100 and 50 nm extruded oleic vesicles suspension (2.2 mM; final total concentration after injection = 4.0 mM). The dilution experiment was done by adding 200 μL of 22 mM NaCl solution into 2.0 mL of a 2.2 mM 50 nm extruded vesicle solution. Each experiment was carried out in triplicate and each curve represents mean values.

conditions, the final size distribution closely resembles that of the preformed vesicles.

Let us consider first the addition of oleate to oleate vesicles. Typical data are summarized in Figure 4, where the vesicle formation is followed by monitoring the optical density of the suspension. Notice that the time course of the vesicles formation in the absence of preformed ones follows a sigmoid trend (curve a), whereas in the case of preadded vesicles, the sigmoid time course still remains although the lag phase is significantly reduced (curves b and c). Consider also that despite the double final surfactant concentration, in the experiments of curves (b) and (c) the final optical density is considerably lower than in (a), and lower for the preadded 50 nm (pore size) extruded vesicles (curve c) than for the 100 nm (pore size) extruded vesicles (curve b).

Photon correlation spectroscopy has then been used to gain insight in the mechanism by following the time evolution of the hydrodynamic average radius and determining the intensity weighted size distributions of aggregates before and after the micelles addition. In Figure 5, the hydrodynamic average radius determined by the cumulant analysis is reported against time in the case of OAV. This plot confirms the observed acceleration in the process due to the preadded aggregates in reaching a final stable size.[18]

Moreover, the graph of Figure 5 shows that in the control experiment (no preexisting vesicles) the formed vesicles have a final average radius larger than in the other case. This accounts for the differences observed in optical density end values, because smaller particles scatter less than larger ones. In the

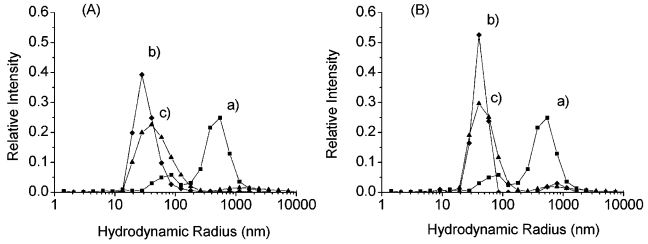

Figure 6. Effect of 50 nm (graph A) and 100 nm (graph B) extruded preadded oleate/oleic acid vesicles on the size distribution of newly formed vesicles. In both graphs, the intensity-weighted size distribution is measured by DLS (scattering angle 90°, 25 °C) before (curves b) and after (curves c) injection of 200 μL of sodium oleate solution (22 mM) into 2.2 mM extruded preformed vesicles, final total concentration = 4.0 mM. The same micellar solution is injected into bicine buffer 0.22 M, pH = 8.5, final surfactant concentration = 2.0 mM (curves a).

cases of 100 and 50 nm extruded vesicles, the final radius values remain close to the initial ones; see Table 1.

In Figure 5, also the result of a simple dilution experiment is reported showing that the hydrodynamic diameter does not change if 200 μL of 22 mM NaCl solution is added to a 50 nm extruded vesicle suspension.[19]

In Figure 6A,B, the intensity-weighted size distributions are compared among the control experiment (curve a) and the 50 and 100 nm extruded preadded vesicles systems, before (curve b) and after (curve c) micelle addition, respectively. First, notice

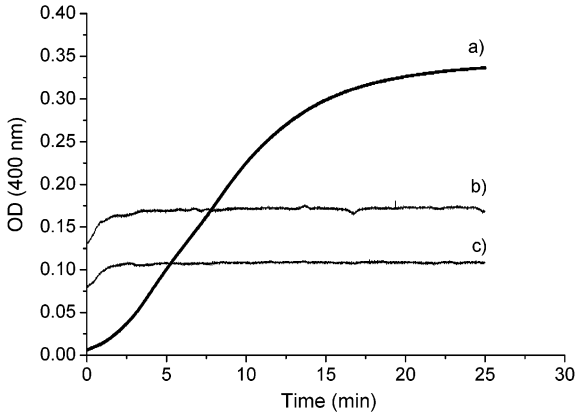

Figure 7. Effect of extruded preadded POPC liposomes on the oleate micelle transformations. The variation of OD after oleate micellar injection into preexisting vesicles is measured by a spectrophotometer (λ = 400 nm, 25 °C). A 200 μL aliquot of sodium oleate aqueous solution (22 mM) is injected into bicine buffer 0.22 M, pH = 8.5, final surfactant concentration = 2 mM (curve a). The same micellar solution is injected into 100 nm (curve b) and 50 nm (curve c) extruded POPC liposome suspension (2.2 mM; final total concentration after injection = 4.0 mM).

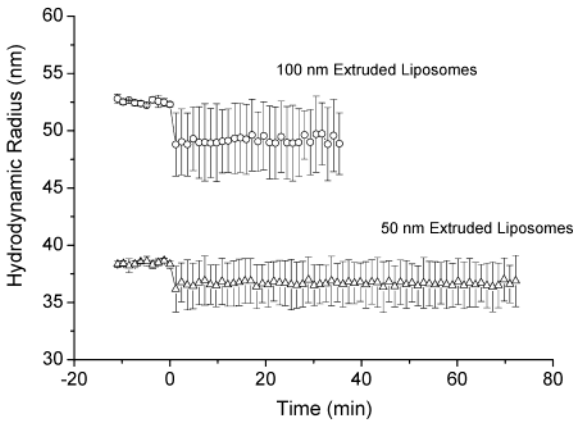

Figure 8. Time progression of hydrodynamic radius before and after injection of oleate micellar solution into extruded preadded POPC liposomes. The radius was measured by DLS (λ = 633 nm, scattering angle 90°, 25 °C). A 200 μL aliquot of sodium oleate aqueous solution (22 mM) is injected into bicine buffer 0.22 M, pH = 8.5, final surfactant concentration = 2.0 mM (control experiment). The same micellar solution is injected into 100 and 50 nm extruded POPC liposome suspension (2.2 mM; final total concentration after injection = 4.0 mM). Each experiment was carried out in triplicate and each curve represents mean values.

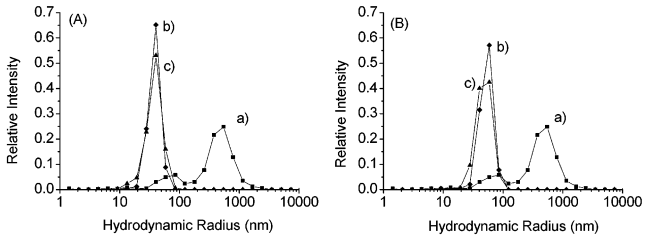

Figure 9. Effect of 50 nm (graph A) and 100 nm (graph B) extruded preadded POPC liposomes on the size distribution of newly formed vesicles. In both graphs, the intensity-weighted size distribution is measured by DLS (scattering angle 90°, 25 °C) before (curves b) and after (curves c) injection of 200 μL of sodium oleate solution (22 mM) into 2.2 mM extruded preformed liposomes, final total concentration = 4.0 mM. The same micellar solution was injected into bicine buffer 0.22 M, pH = 8.5, final surfactant concentration = 2 mM (curves a).

the dramatic difference between the final bimodal size distribution in the control experiment (curve a), with a small peak centered on about 80 nm and a larger peak on about 500 nm, and the final sharp distributions in the presence of preadded aggregates (curves c in Figure 6A,B). Furthermore, the size distributions (b) and (c) are very similar to each other for both extruded vesicles sizes, and in particular, the initial ones appear to be widened and shifted to large values by the micelle addition. This is also confirmed by data in Table 1, obtained by cumulant analysis.

Aside from the matrix effect, there is another general observation stemming from Table 1: this is the significant difference between the expected radius (corresponding to the filter pores diameter) of the extruded vesicles or liposomes and the observed ones. In fact, if the filter pore diameter is larger than 100 nm, the measured radii of extruded liposomes are generally smaller than expected. However, for pore diameter of 50 nm,[14] the measured liposome radius is higher than the pore size. A similar trend can also be found for oleate extruded vesicles. As is well-known, vesicle would relax to the minimum energy size if they were equilibrium systems and would instead acquire the size of the filter pore if they would be mechanically constrained into kinetic traps. The mixed behavior observed in our case suggests, as already pointed out elsewhere,[20] that the system is not a real equilibrium system.

The addition of detergent to a preformed suspension at different molar ratios was also investigated (data not shown). Ratios either with an excess of surfactant or an excess of preexisting vesicles were considered by keeping constant the final total concentration. It is interesting to note that the final optical value was lower at all ratios than in the control experiment despite the same final concentration. Furthermore, by decreasing the concentration of the surfactant forming the preformed vesicles, the process showed a behavior similar to the control experiment, and the stable value was reached more slowly. Dynamic light scattering experiments revealed that in all cases the radius exhibited a tendency to rise after injection but remained low with regard to the value achieved in the control experiment.

Let us consider now the case of oleate added to extruded POPC liposome. Under these conditions, as amply documented in the literature,[21] oleate is rapidly absorbed by the POPC liposomes and mixed oleate/POPC liposomes are built. Figure 7 shows the OD time progress after micelles addition, which is similar to what is observed in Figure 5. When the same amount of oleate is added to aqueous suspensions of 50 and 100 nm extruded POPC liposomes, the formation of new mixed liposomes is extremely rapid and actually the initial time progress is lost during the dead time of the experiment. A plateau of the optical density difference is reached in both cases (curve b and c in Figure 7) within 1−2 min, against the 5−6 min of the control experiment. Note again that the final optical density is smaller when preadded POPC liposomes are present. The time evolution of the average hydrodynamic radius, reported in Figure 8, shows a small decrement in the aggregate size after micelle injection,[22] and with respect to the preadded OAV, larger fluctuations (error bars) are observed.

Let us consider now the final size distributions, illustrated in Figure 9A,B, in the case of 50 and 100 nm extruded POPC preadded liposomes, respectively. The first observation is again the significant difference between the final bimodal size distribution in the control experiment (curve c) and the sharp peaks obtained after micelle injection to POPC liposomes (curves b). Moreover, in both 50 and 100 nm extruded POPC cases, the final size distribution (curve c) results slightly widened

and shifted toward lower values with respect to the initial one, as confirmed by the cumulant analysis data collected in Table 1.

Particularly interesting is the comparison between the cases of preformed liposomes and vesicles. In fact, although both of them exhibit the matrix effect, there is no evidence of the growth of liposomes in contrast to the case of vesicles, as apparent from data in Table 1.

Size Accretion and the Population Increase. Can one provide a more quantitative interpretation of the data of Table 1? We will attempt to do so in this section. Let us consider first again Figure 1. Accordingly, as already mentioned, there are different possible mechanisms for the micelles transformation upon addition of new amphiphiles to a solution containing preformed vesicles: either the production of new vesicles independently of the preexisting ones (uncooperative mechanism) or the production of vesicles based on an accretion and an eventual division of the preexisting ones (cooperative mechanism). Therefore, the micelle transformation in the presence of preexisting vesicles can result both in a size accretion and a population increase independently on the involved mechanism. In the case of a 1:1 addition of fresh surfactant, for instance if only a uniform accretion mechanism were operative, the total surface would increase by a factor of 2, which means that the average radius of the vesicles would increase by a factor $\sqrt{2}$, whereas the number of particles and the polydispersity index[23] would remain constant. Conversely, if the average radius and the polydispersity of the preexisting vesicles would not change, then the number of particles would be doubled. To quantify these two possible effects, it is useful to introduce two index parameters[24] in terms of the squared average radius $\bar{R}^2$ and the size distribution variance σ^2. In particular we will make use of the index of size

$$f_R = \frac{1}{c}\left(\frac{\bar{R}_{end}^{\ 2} + \sigma_{end}^{\ 2}}{\bar{R}_0^{\ 2} + \sigma^2_0} - 1\right) \tag{1}$$

and the index of population

$$f_N = \frac{\bar{R}_0^{\ 2} + \sigma^2_0}{\bar{R}_{end}^{\ 2} + \sigma_{end}^{\ 2}}(1 - f_R) \tag{2}$$

where the labels "0" and "end" indicate values before and after the addition, respectively. The constant c represents the ratio $(a_2[S_2])/(a_1[S_1])$ between the product of the concentration $[S_i]$ times the polar head area a_i of the added surfactant molecules ($i = 2$), divided by those of the preexisting amphiphiles ($i = 1$). These indices were obtained for spherical shaped aggregates of negligible bilayer thickness assuming that all the surfactant molecules are present in solution as vesicles or liposomes.[25] In fact, under these assumptions, the total surface area of vesicles per unit of concentration $a_2[S_2] + a_1[S_1]$ can be equated to the integral:

$$a_1[S_1] + a_2[S_2] = \int [V]8\pi R^2 P(R)\, dR = 8\pi(\bar{R}^2 + \sigma^2)[V]$$

where [V] is the vesicle−liposome concentration, $P(R)$ is the aggregate size distribution, and $8\pi R^2$ is the surface area of a bilayered spherical vesicle of radius R. It is possible to demonstrate that if all the new amphiphiles are absorbed by the preexisting aggregates, without forming new vesicles (*size accretion only*), the two indices become $f_N = 0$ and $f_R = 1$. Conversely, if the added molecules simply increase the population of the preexisting aggregates, without changing the average radius and polydispersity of the size distribution (*population increase only*), then it will give $f_N = 1$ and $f_R = 0$. It should be stressed that these two indices provide only an insight of the final state of the systems and not of the involved mechanisms.[26]

In Table 1, the values of these indexes are calculated for the cases investigated in this work. The question is whether and to what extent the observed matrix effect data can be explained in terms of the accretion and/or population increase.

Let us consider first the case of 50 nm extruded oleate vesicles. Here, all the surfactant addition results in an increase in size and polydispersity of the preexisting aggregates. In the case of 100 nm extruded oleate vesicles, both index values are between 0 and 1 and this implies that the behavior of these aggregates cannot be reduced only to the accretion effect. In this case both an increase of size and an increase of number of particles must be operative.

Conversely, in both cases of POPC liposomes, it appears that the population increase is operative. In these last two cases, $f_N > 1$ means that the number of particles is increased a little more than what predicted assuming a constant size distribution. This, in turn, suggests a fission of the preexisting liposomes caused by a perturbation due to the binding of the added oleate micelles, as confirmed by $f_R < 0$ and by the smaller final radius. To account physically for this, it is important to recall that, because POPC molecules are zwitterionic surfactants, liposome membranes are globally uncharged, whereas oleate vesicle membranes become negatively charged. Therefore, the uptake of oleate/oleic acid droplets by liposomes will be faster than vesicles due to the electrostatic repulsions among carboxylate molecules in the second case. Moreover, this fast uptake of charged molecules can perturb liposomes by creating an asymmetric distribution of charge on the outside layer of the membrane. As already mentioned, independent experimental evidence of this aggregate fission has been recently obtained by means of cryotransmission electron microscopy investigations with ferritin-labeled liposomes.[8]

Simple Model for the Cooperative Mechanism. In the previous sections, we have seen that the formation of oleate vesicles or mixed POPC/oleate vesicles is characterized by a cooperative behavior, and that the presence of preformed vesicles significantly alters the time course of vesicle formation, as well as their size distribution. In this section, we focus attention on the cooperative behavior to demonstrate that it cannot be described by a simple first-order transition mechanisms and that an autocatalytic second-order step has to be introduced to reproduce this feature.

In recent years, the time evolution of the micelle−vesicle transformation has been studied using different techniques, such as turbidity measurements,[27,28] dynamic light scattering,[28,29] and fluorescence probe encapsulation,[28] and despite the complexity of the process the data analysis has often been based on simplified first-order kinetic models. Typical studies are those by Robinson et al.[29a] and Connor and Hatton.[30a]

Different mechanisms and different intermediate structures have been supposed for the micelle−vesicle transformation. Rodlike micelles, bilayer fragments, and open vesicles are hypothesized to be involved in the structural rearrangements of cholesterol−lecithin vesicles exposed to bile salts.[28] Robinson[29] suggested disklike structures, and small size vesicles and disks were postulated[30a,30,31] and observed[30b] under certain conditions in the case of cetyltrimethylammonium bromide (CTAB) and sodium octyl sulfate.

Concerning the addition of oleate micelles into a buffered solution at pH 8.5, it is then plausible that spherical micelles

transform into disklike aggregates composed of oleate and oleic acid molecules in agreement with titration experiments.[11,32] These lamellar aggregates self-assemble and eventually form closed bilayer spherical structures to minimize the contact between the hydrocarbon chains on the edge and water.[33] In this framework, the micelle−vesicle transition can be described by using a simple pseudo-first-order mechanism:

$$\mathrm{M} \xrightarrow{k_1} \mathrm{L} \xrightarrow{k_2} \mathrm{V} \tag{3}$$

Equations 3 represents a chain of transformations among different phases: micelles M, lamellar intermediates L, and vesicles V. This simple kinetic pathway without cooperative behavior will be called mechanism I. The rate of each step is assumed proportional to the surfactant concentration and to relative apparent kinetic constant.

A cooperative step can be inserted as follows:

$$\mathrm{M} + \mathrm{V} \xrightarrow{k_3} n\mathrm{V} \tag{4}$$

where (assuming $n > 1$) M and V interact to give more V in a kind of autocatalytic process ($n = 2$ in this oversimplified treatment). The coupling of eqs 3 and 4 gives rise to a mechanism II. To get the time evolution of the surfactant molar fractions, χ_M, χ_L, and χ_V according to this mechanism, the following dimensionless ordinary differential equation set has to be solved:

$$\frac{1}{S_0 k_1}\frac{\mathrm{d[M]}}{\mathrm{d}t} = \frac{\mathrm{d}\chi_M}{\mathrm{d}(tk_1)} = -\chi_M - \left(\frac{k_3 S_0}{k_1}\right)\chi_M\chi_V \tag{5a}$$

$$\frac{1}{S_0 k_1}\frac{\mathrm{d[L]}}{\mathrm{d}t} = \frac{\mathrm{d}\chi_L}{\mathrm{d}(tk_1)} = +\chi_M - \frac{k_2}{k_1}\chi_L \tag{5b}$$

$$\frac{1}{S_0 k_1}\frac{\mathrm{d[V]}}{\mathrm{d}t} = \frac{\mathrm{d}\chi_V}{\mathrm{d}(tk_1)} = +\frac{k_2}{k_1}\chi_L + (n-1)\left(\frac{k_3 S_0}{k_1}\right)\chi_M\chi_V \tag{5c}$$

This set has been solved numerically using a Runge−Kutta method of fourth order, where S_0 is the overall surfactant molecules concentration: $S_0 = [M_0] + [V_0]$.

Mechanism I can be solved analytically and the time course of the vesicle formation χ_V as a function of time is

$$\chi_V = \chi_V^0 + \chi_M^0\left(1 + \frac{k_1\exp(-k_2 t) - k_2\exp(-k_1 t)}{k_2 - k_1}\right) \tag{6}$$

By mechanism I, a sigmoidal trend for χ_V can be obtained only if $k_2/k_1 \approx 1$, i.e., if the intermediate has a lifetime comparable to the length of the process (see Figure 10, dashed curve b). In fact, if $k_2 \ll k_1$ micelles quickly convert into intermediates that are relatively stable, so that the rate determining step is the transformation of L into V (see Figure 10, dashed curve c) and eq 6 becomes

$$\chi_V = \chi_V^0 + \chi_M^0[1 - \exp(-k_2 t)]$$

On the other hand, if $k_2 \gg k_1$, i.e., the formation of the intermediates is the rate determining step (dashed curve a), then eq 6 simply reduces to the decay of micelles:

$$\chi_V = \chi_V^0 + \chi_M^0[1 - \exp(-k_1 t)]$$

When no vesicles are present at the beginning, to obtain a sigmoid trend according to mechanism II, due to the cooperative step the following condition has to be verified:

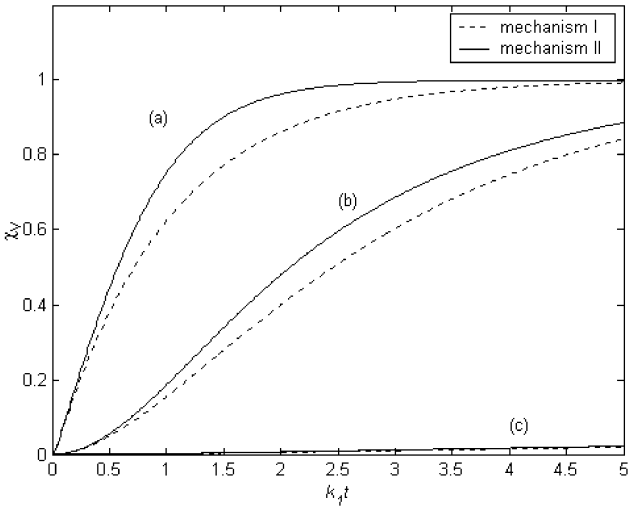

Figure 10. Time evolution of vesicles molar fraction calculated according to mechanism I, eq 3 (dashed curves), and mechanism II, eqs 3 and 4 (solid curves). All curves are determined by setting the initial conditions $\chi_M^0 = 1.0$, $\chi_L^0 = \chi_V^0 = 0.0$ and the ratio $(k_3C/k_1) = 1.0$, whereas (k_2/k_1) equals 50 (a), 0.5 (b), and 0.005 (c). Dashed curves are the plots of eq 6, and solid curves have been obtained numerically by solving the set of ordinary differential equations (5a)−(5c).

$$\frac{R_B}{S_0} = \left(\frac{k_3 S_0}{k_1}\chi_M\chi_V\right) \geq \frac{R_F}{S_0} = \left(\frac{k_2}{k_1}\chi_L\right)$$

where R_B is the micelle binding rate and R_F is the vesicle formation rate.

This means that according to the differential equation (5c) the micelle cooperative transformation contribution must be greater than or equal to the intermediate conversion rate. In terms of the kinetic constant, this condition can be approximated as follows:

$$\left(\frac{k_3 S_0}{k_1}\right) \geq \frac{k_2}{k_1} \geq 1$$

In Figure 10, only case b (solid curve) satisfies the last inequality. Conversely, in case c, $k_2/k_1 \ll 1$, both mechanisms give a coincident outcome, because micelles quickly transform into the intermediates that slowly form vesicles and, when vesicles appear in solution, micelles are no longer present. Figure 11 shows the transition between an exponential trend to sigmoidal one as the ratio (k_3S_0/k_1) becomes greater than k_2/k_1. When $(k_3S_0/k_1) = 0.1 \ll (k_2/k_1) = 50.0$ no cooperative behavior is exhibited by the system and mechanism II practically reduces to mechanism I. On the other hand, when vesicles are already present at the beginning, only mechanism II can correctly predict the observed change from a sigmoidal trend to an exponential growth (see Figure 12), whereas mechanism I can predict solely a shift toward high values of the sigmoidal profile, as clearly shown by eq 6.

In conclusion, the simple kinetic model presented here shows that the cooperative behavior observed in the oleate micelle−vesicle transformation can be explained only if a second-order autocatalytic step is taken into account.

Clearly, such a kinetic model cannot describe the single molecular events accompanying accretion or fission. The picture implied here is simply a fusion of micelles with the preexisting vesicles. Moreover, due to the abrupt pH change it is not possible to exclude that micelles, alternatively, can at least in

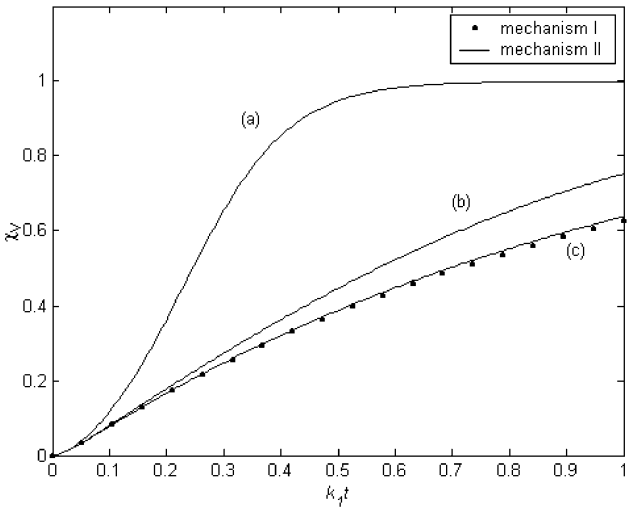

Figure 11. Time evolution of vesicles molar fraction calculated according to mechanism I, eq 3 (points), and mechanism II, eqs 3 and 4 (solid curves). All curves are determined setting the initial conditions $\chi_M^0 = 1.0$, $\chi_L^0 = \chi_V^0 = 0.0$ and the ratio $(k_2/k_1) = 50$, whereas (k_3C/k_1) equals 10 (a), 1.0 (b), and 0.1 (c). Points are obtained as the plots of eq 6 and solid curves have been obtained numerically by solving the set of ordinary differential equations (5a)−(5c).

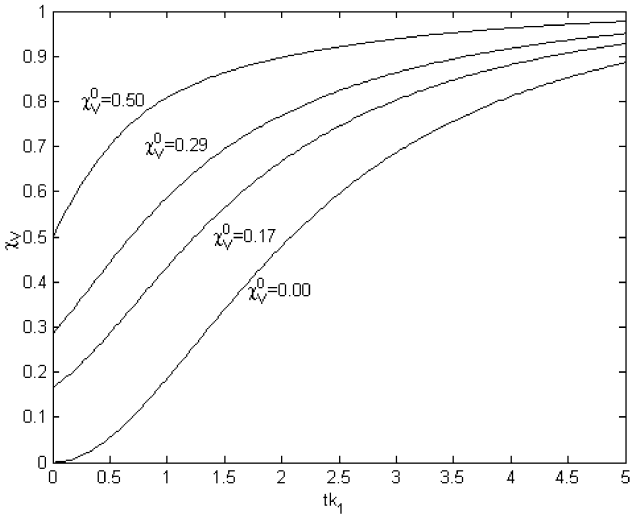

Figure 12. Time evolution of vesicles molar fraction calculated according to mechanism II, eqs 3 and 4. All the curves are determined numerically by solving the ordinary differential equations set (5a)−(5c) and setting $(k_2/k_1) = 0.5$ and $(k_3C/k_1) = 1.0$, and for the initial conditions $\chi_M^0 = 1.0$, $\chi_L^0 = 0.0$ whereas χ_V^0 values are reported on the plot.

part form small droplets with a fatty acid core and oleate on the boundary.[10] These droplets, stable at higher pH values,[33] can represent a reserve of material that allows the growth of the more stable vesicular aggregates at very long time.

Concluding Remarks

The question of the self-reproduction of fatty acid vesicles is of general interest for the field of aggregate compartmentation and has in addition a particular interest in the prospect of prebiotic chemistry. In fact, in this field one would like to know whether these simple vesicular structures might be able to reproduce under prebiotic conditions, i.e., prior to the development of refined biochemical machineries based on enzymes and nucleic acids. The question is then whether physical factors and simple thermodynamic constraints can induce growth, fission, and self-reproduction of vesicles.

In this paper the time evolution of the oleate micelle−vesicle transformation due to an abrupt pH change has been investigated, focusing the attention on the matrix effect that arises when an oleate micelle solution is injected into a suspension of preformed vesicles or liposomes. This phenomenon, previously described, has been reinvestigated here, and it has been ascribed to a cooperative micelle binding to a vesicle, as schematically illustrated in Figure 1. The micelle binding accelerates the micelle−vesicle transformation as confirmed by the OD time evolution. Moreover, this work has contributed to a better understanding of the basic processes: the size accretion and the population increase of vesicles that can take place as a consequence of the micelle binding. In particular, it has been possible by means of dynamic light scattering analysis to follow the time change of the vesicle average radius occurring upon addition of fresh surfactant and also to assess the relative increment of the particle concentration. In particular, in the case of oleate added to POPC it has been possible to estimate an increase of the vesicle concentration that confirms processes of fission, which (except for a publication form in our own group) has never been observed before in the literature. It is therefore apparent that fatty acid vesicles can undergo processes of growth, fission, and self-reproduction depending on rather simple external conditions. As mentioned earlier, this may be important for understanding the development of early protocells.

The theoretical model developed here has the characteristic of great simplicity; and despite this, it is possible to describe the cooperative mechanism of autocatalytic growth of vesicles. The prerequisite for that is the binding of micelles to preexisting vesicles to give more vesicles—a mechanism that has been formulated qualitatively a number of times, never, however, described in an analytical form.

This theoretical model leaves of course the main questions of the chemical mechanism. Why and how do preexisting vesicles increase the velocity of formation of novel vesicles (a kind of catalysis), determining at the same time their form in such a way that the final size distribution is very similar to the initial one? Why and how do mixed oleate/POPC vesicles divide to yield smaller ones? Can these properties observed for fatty acid vesicles be shared by other types of surfactants, for example, positively charged ones and/or neutral ones?

These questions will form the bulk of work for further studies in our group.

References and Notes

(1) Bachmann, P. A.; Luisi, P. L.; Lang, J. *Nature* **1992**, *357*, 57−59.
(2) Morigaki, K.; Dallavalle, S.; Walde, P.; Colonna, S.; Luisi, P. L *J. Am. Chem. Soc.* **1997**, *119*, 292−301.
(3) Walde, P.; Wick, R.; Fresta, M.; Mangone, A.; Luisi, P. L *J. Am. Chem. Soc.* **1994**, *116*, 11649−11654.
(4) Wick, R.; Walde, P.; Luisi, P. L.; Fleischaker, G. R.; et al. *Self-reproduction of Supramolecular structures*; Kluwer Academic Publishers: Amsterdam, 1994; pp 225−259.
(5) Wick, R.; Walde, P.; Luisi, P. L *J. Am. Chem. Soc.* **1995**, *117*, 1435−1436.
(6) VonMont-Bachmann, P.; Walde, P.; Luisi, P. L. *J. Liposome Res.* **1994**, *4* (3), 1135−1158.
(7) (a) Blöchliger, E.; Blocher, M.; Walde, P.; Luisi, P. L *J. Phys. Chem. B* **1998**, *102*, 10383−10390. (b) Lonchin, S.; Luisi, P. L.; Walde, P.; Robinson B. H. *J. Phys. Chem. B* **1999**, *103*, 10910−10916.
(8) (a) Berclaz, N.; Müller, M.; Walde, P.; Luisi, P. L *J. Phys. Chem. B* **2001**, *105*, 1056−1064. (b) Berclaz, N.; Blöchliger, E.; Müller, M.; Luisi, P. L *J. Phys. Chem. B* **2001**, *105*, 1065−1071.
(9) Small, D. M. The *Physical Chemistry of Lipids*; Handbook of Lipid Research 4; Plenum Press: New York, 1986.
(10) Fukuda H.; Goto A.; Yoshioka H.; Goto R.; Morigaki K.; Walde P. *Langmuir* **2001**, *17*, 4223−4231.
(11) Cistola, D. P.; Atkinson, D.; Hamilton, J. A.; Small, D. M. *Biochemistry* **1986**, *25*, 2804−2812. (b) Cistola, D. P.; Hamilton, J. A.; Jackson, D.; Small, D. M. *Biochemistry* **1988**, *27*, 1881−1888.

(12) In fact, it should also be recalled that the optical density depends both on the number and on the squared volume of the scattering particles; see Materials and Methods for further details.

(13) Mayer, L. D.; Hope, M. J.; Cullis, P. R. *Biochim. Biophys. Acta* **1986**, *735*, 161−168.

(14) Matsuzaki, K.; Murase O.; Sugishita, K.; et al. *Biochim. Biophys. Acta* **2000**, *1467*, 219−226.

(15) Koppel, D. E. *J. Chem. Phys.* **1972**, *57*, 4814.

(16) Provencher, W. *Comput. Phys. Commun.* **1981**, *27*, 213.

(17) Berne, B. J.; Pecora, R. *Dynamic Light Scattering*; Wiley: New York: 1976.

(18) It is worthwhile to mention that at long time (after some days) some rearrangements also occur, the studied systems not being at equilibrium.

(19) Same results were obtained for 100 nm extruded vesicles as well as for 50 and 100 nm extruded liposomes (data not shown).

(20) Luisi, P. L. *J. Chem. Educ.* **2001**, *78* (3), 380−384.

(21) (a) Hamilton, J. A.; Cistola, D. P. *Proc. Natl. Acad. Sci. U.S.A.* **1986**, *83*, 82. (b) Kamp, F.; Hamilton, J. A. *Proc. Natl. Acad. Sci. U.S.A.* **1992**, *89*, 11367. (c) Kamp, F.; Zakim, D.; Zang, F.; Noy, N.; Hamilton, J. A. *Biochemistry* **1995**, *34*, 11928. (d) Kleinfeld, A. M.; Chu, P.; Romero, C. *Biochemistry* **1997**, *36*, 14146. (e) Hamilton, J. A. *J. Lipid Res.* **1998**, *39*, 467.

(22) The first hydrodynamics radius required 2 min to be determined by the light scattering equipment.

(23) For a given vesicle suspension of average radius $-R$ and variance σ^2 the polydispersity index P is defined as $P = s^2/\bar{R}^2$.

(24) Rasi, S.; Mavelli, F.; Luisi, P. L. *Origins of Life and Evolution of the Biosphere*, submitted for publications.

(25) A less restrictive requirement is that the fraction of amphiphiles present as vesicles remain the same at the beginning and at the end of the process.

(26) In the case of an exclusive size accretion, the binding of the fresh surfactants can be invoked, whereas if only the population increases the uncooperative mechanism cannot be in principle excluded. On the other hand, the process acceleration observed suggested that the cooperative micelle binding has to take place and therefore the population increase observed can be ascribed to splitting processes of the growing vesicles.

(27) Luk, A. S.; Kaler, E. W.; Lee, S. P. *Biochemistry* **1997**, *36*, 5633−5644.

(28) (a) Robinson, B. H.; Bucak, S.; Fontana A. *Langmuir* **2000**, *16*, 8231−8237. (b) Farquhar, K. D.; Misran, M.; Robinson, B. H.; Steytler, D. C.; Morini, P.; Garrett, P. R.; Holzwarth, J. F. *J. Phys.: Condens. Matter* **1996**, *8*, 9397.

(29) (a) O'Connor, A. J.; Hatton, T. A.; Bose, A. *Langmuir* **1997**, *13*, 6931−6940. (b) Xia Y., Goldmints I.; Johnson P. W.; Hatton T. A.; Bose A. *Langmuir* **2002**, *18*, 3822−3828.

(30) Fromherz, P. *Chem. Phys. Lett.* **1983**, *94*, 259−266.

(31) Somoza, A. M.; Marconi, U. M. B.; Tarazona, P. *Phys. Rev. E* **1996**, *53*, 5123−5129.

(32) See, for instance: Small, D. M. The *Physical Chemistry of Lipids*; Handbook of Lipid Research 4; Plenum Press: New York, 1986; pp 296−299.

(33) Experimental evidence of the formation of these intermediate structures in the cationic micelle−vesicle transformation have been recently reported: Fromherz, P. *Chem. Phys. Lett.* **1983**, *94*, 259−266.